Architecture of the Ti(IV) Sites in TiAlPO-5 Determined Using Ti K-Edge X-ray Absorption and X-ray Emission Spectroscopies

UNIVERSITÀ DEGLI STUDI DI TORINO

The architecture of the Ti(IV) sites in TiALPO-5 determined using Ti K-edge X-ray absorption and X-ray emission spectroscopies

Erik Gallo[*a] *Andrea Piovano,*[*b] *Carlo Marini,*[a] *Olivier Mathon,*[a] *Sakura Pascarelli,*[a] *Pieter Glatzel,*[a] *Carlo Lamberti,*[c,d,e] *and Gloria Berlier,*[c]

[a] European Synchrotron Radiation Facility (ESRF) 6 Rue Jules Horowitz, BP 220 38043 Grenoble Cedex 9 France.

[b] Institut-Laue-Langevin (ILL) 6 Rue Jules Horowitz, BP 220 38043 Grenoble Cedex 9 France.

[c] Department of Chemistry, INSTM Reference Center and NIS Centre of Excellence, Università di Torino, Via P. Giuria 7, I-10125 Torino, Italy.

[d] CrisDI Center for Crystallography, University of Turin, Italy

[e] Southern Federal University, Zorge street 5, 344090 Rostov-on-Don, Russia

KEYWORDS. AlPO, XAFS, EXAFS, XES, Titanium substituted aluminophospate, DFT

ABSTRACT. X-ray absorption and emission spectroscopies, supported by quantum mechanical calculations were used to determine the architecture of Ti(IV) sites in Ti aluminophosphate $AlPO_4$-5. The chemical sensitivity of the $K\beta_{2,5}$ X-ray emission lines of Ti(IV) was exploited to monitor its local environment, proving that it mainly substitutes P(V) in the framework, with a

not negligible fraction substituting Al. Local structure of the substituted sites was found to be considerably deformed with respect to the $AlPO_4$-5 original framework.

1 Introduction

Molecular sieves (MS) are of paramount importance in many fields of science and technology.[1-4] In particular, aluminosilicates MS are of great significance in heterogeneous catalysis.[5] Titanium silicalite-1 (TS-1)[6-8] developed by Eni is one of the most investigated metal substituted MS and it is of primary importance in the petrochemical industry.[1] The discovery of the extraordinary properties of TS-1 pushed the research in this field towards the development of other Ti-substituted MS having different framework composition and structure and thus diverse selectivity and activity.[9-13]

Since form the pioneering report by Wilson et al.[14] it was evident that many topological structures typical of zeolitic materials can be achieved with strictly alternating Al and P tetrahedral framework sites. This allowed the development of a variety of MeAlPO and SAPO structures doped with transition metal or Si ions, respectively.[15-21] One important material of this series is based on Ti(IV) substituted AlPO catalyst, showing 1) higher microporous diameter and 2) superior hydrophilicity with respect to TS-1.[5,22,23] TiAlPO-5 - a Ti substituted AlPO with the AFI framework - fulfils these requirements.

The local environment and the electronic properties of the Ti sites within the structure of TiAlPO-5 were explored using various spectroscopic techniques.[24-27] Nevertheless, contradictory results on the preferential substitution site of Ti ions are present in literature. On the basis of ^{27}Al and ^{31}P MAS NMR experiments, Akolekar et al.[24] proposed that Ti(IV) mainly substituted for P sites in an AFI framework with negligible presence of extraframework Al, P, Ti elements. On the same advice were Prakash et al.[27,28] who claimed that Ti ions are located at P framework sites in

various TAPOs, on the basis of ESR (electron spin resonance) and ESEM (Electron spin-echo modulation) measurements of Ti(III) species produced by γ -ray reduction. More accurate EPR and HYSCORE (hyperfine sublevel correlation) measurements by Maurelli et al.[25,26] recently provided direct evidence for framework substitution of reducible Ti ions at Al sites, in a TiAlPO-5 catalysts mildly reduced with H_2. It is worth noticing here that experiments performed probing electrons spin rely on the signal from Ti(III) species only, which are obtained after specific reduction processes.

Density functional theory (DFT) simulation techniques were also employed to describe the electronic properties and bonding ionic nature in Ti substituted AlPO-5 systems, but also in this case contrasting views are found in the literature. For instance, Elanany et al.[29] discussed a model with Ti(IV) replacing one of the framework pentavalent phosphorous ions, with a compensating proton stabilized to the neighboring oxygen atom. On the contrary Corà et al.[30] found that the ionic character of the Al-O interaction is likely to control the defect chemistry of the Al site. This implies that ionic substitutional dopants causes only a mild perturbation to the host electronic structure when replacing Al ions, suggesting a preferential substitution of these sites withrespect to P.

In the frame of this unclear picture, we decided to use two bulk element sensitive selective techniques in order to precisely investigate the local environment of Ti(IV) ions in thermally activated TiAlPO-5 samples (hereafter TiAlPO-5/act). Namely, extended X-ray absorption fine structure and valence to core X-ray emission spectroscopy, EXAFS[31-33] and vtc-XES, respectively were employed.[34,35] EXAFS allowed us to obtain information on the Ti coordination number and Ti-ligand bond-lengths while vtc-XES was able to identify first and second shell

ligands.[36] Our interpretation of the experimental data relies on ground state DFT calculations performed on appropriate cluster models.

2 Experimental

2.1 Sample Preparation

TiALPO-5 and TS-1 samples were synthesized according to Ref. [25] and Refs. [36,37], respectively. Before measurements samples were calcined and subsequently activated at 673 K to remove water and other adsorbed molecules. We refer to these samples as TiALPO-5/act and TS-1/act, respectively.

2.2 Techniques

The X-ray spectroscopy experiments were performed at ID26 and BM23 beamlines of the European Synchrotron Radiation Facility (ESRF, France).

The Ti K-edge HERFD XANES[38] and the valence to core X-ray emission measurements[39] were performed at ID26. The incident energy was selected by means of a pair of cryogenically cooled Si(111) single crystals. Higher harmonics were suppressed by three Si mirrors operating in total reflection. The beam size on the sample was approximately 1.0 mm horizontally and 0.2 mm vertically. The spectrometer of ID26 exploits the (331) Bragg reflection of five spherically bent Ge crystals (radius 1000 mm) arranged in a vertical Rowland circle geometry. The emitted photons, selected by the spectrometer, were detected using an avalanche photo-diode. The total energy bandwidth was 0.9 eV. The vtc-XES spectra were measured by tuning the incident energy above the Ti K-edge at 5015 eV and scanning the emitted energy. All data are normalized to the

spectral area that includes the Kβ main and the vtc lines (4910 eV – 4975 eV). The background from the $K\beta_{1,3}$ emission line tail was subtracted by fitting four Voigt line profiles. Details about this procedure can be found elsewhere. The HERFD-XANES spectra were collected at the maximum of the $K\beta_{1,3}$ main line and normalized to the edge jump.[36]

The Ti K-edge EXAFS spectra were collected in fluorescence mode at BM23 equipped with a Si(111) double crystal monochromator. A Silicon stripe double mirror was employed to reject higher harmonics. The incoming photon flux was measured using a ionization chamber (filled with nitrogen gas). The fluorescence was recorded using a thirteen element solid state Ge detector. The beam size on the sample was 2.5mm in horizontal and 0.5 mm in vertical. The extraction of the χ(k) function was performed using the Athena code.[40] For each sample, five consecutive EXAFS spectra were collected and corresponding χ(k) functions were averaged before data analysis to obtain a sufficient signal to noise ratio.[41] EXAFS data analysis was performed using Arthemis software.[40] Phase and amplitudes were calculated by the FEFF6 code[42] using cluster models presented hereafter. For The averaged $k^2\chi(k)$ function was Fourier transformed in the Δk = 1.00-9.00 $Å^{-1}$ interval.

On both beam-lines the sample was measured in vacuum inside a cell oriented at 45° with respect to the incident beam.

2.3 Theoretical Methods

Starting from the crystallographic structure presented in Ref. 14, two tetrahedral clusters of twenty-one atoms, with Ti substituting the central (Al or P) atom were built. Dangling bonds were saturated with H. The dimension of these clusters (*i.e.* number of atoms) is thus thirty-three

which is a good compromise of CPU time and accuracy[36] The two clusters can be written as $[Ti(OAl(OH)_3)_4]^{4-}$ (***MAl***) and $[Ti(OP(OH)_3)_4]^{4+}$ (***MP***) and are shown in Figure 1.

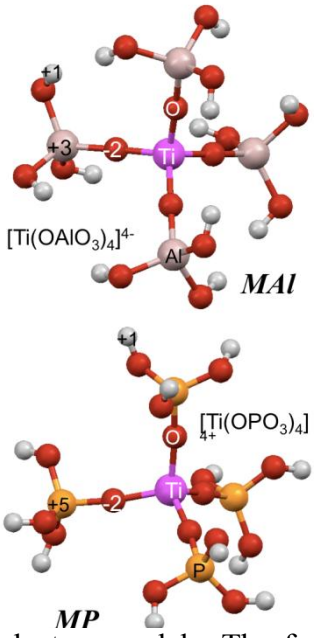

Figure 1. ***MAl*** and ***MP*** optimized clusters models. The formal charge on Ti is +4 while it is indicated for the other ions.

These clusters are analogous to the $[Ti(OSi(OH)_3)_4]^{4-}$ used by Ricchiardi et al.[43] and by Damin et al.[44] (cluster named T5 in that work) to simulate the local environment of Ti(IV) in TS-1 framework. The geometry of these models was optimized by DFT calculations, while the vtc-XES spectra were simulated with the ORCA program system.[45] The CP(PPP)and TZVP basis sets were adopted for Ti and its ligands, respectively, according to previous works.[36,46] Several density functionals (BP86, PWP, OLYP, B1LYP, B3LYP, PBE0 and TPSSh), moving from gradient corrected to hybrid gradient corrected functionals, were used to check the effect of various level of theory.

The cluster model $Ti[OSi(OH)_3]_4$ is representative for the local environment of TS-1 and it was optimized using the TPSSh/TZVP/CP(PPP) level of theory according to Ref. [36] Six clusters

where the Ti-O (first shell) bond length is set to 1.75 Å up to 2.00 Å were thus built. The structures and corresponding molecular orbitals were plotted using the software UCSD Chimera.[47]

3 Results and Discussion

One of the explanations for the different results reported in literature (see Introduction) could be ascribed to the different treatments undergone by the samples. Indeed reduction processes on a TiALPO-5/act (carried out to check redox phenomena or to obtain EPR active Ti(III) sites) can result in a modification of the cation bonding geometry. To shed some light on this aspect the Ti K-edge high energy resolution fluorescence detected (HERFD) X-ray absorption near edge structure (XANES) spectra of TiAlPO-5/act and TiALPO-5/ act reduced with H_2 are reported in Figure 2. It is well known that XANES is sensitive to the electronic and geometric structure of the metal sites.[32,33,48] From Figure 2 it is possible to see that the reduction process affects the spectrum of TiALPO-5/act.

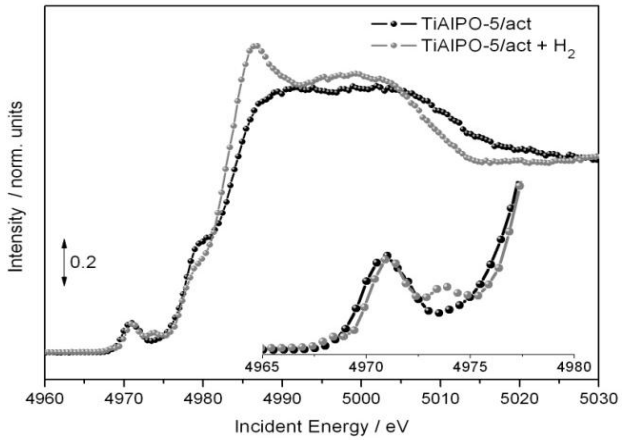

Figure 2. High energy resolution fluorescence detected (HERFD) XANES acquired at the maximum of the Kβ main line: TiALPO-5/act (black curve) and TiALPO-5/act reduced with H_2 (gray curve).

DFT was employed to optimize the model clusters reported in Figure 1, with Ti(IV) substituting an Al site (***MP***) or a P site (***MAl***). These were employed to calculate the theoretical paths to be employed in the Ti K-edge extended X-ray absorption fine structure (EXAFS) analysis and to calculate the vtc-XES spectrum and involved orbitals.

The EXAFS oscillations of TiALPO-5/act are reported in Figure 3a, with the corresponding modulus and the imaginary part of the Fourier Transform signal in Figure 3b and Figure 3c, respectively. Only a first shell single scattering path from oxygen atoms was considered in the fit of the EXAFS oscillations (blue curve; fit in the ΔR = 0.80-2.00 Å range, in Figure 3a). On the contrary, second shell paths and multiple scattering MS contributions were considered to fit the FT signals in Figure 3b,c (green curve fit for ***MP*** model, red curve for ***MAl*** one; fits in the ΔR = 0.80-3.80 Å range).

Table 1. Report of the Most Important Parameter Obtained by Fitting the First Shell (Ti-O) and second shell (Ti-M, M=Al,P) contribution of Ti-AlPO-5, using models MP and MAl to compute theoretical paths.

Model	S_0^2	ΔE_0	R (Ti-O)	σ^2 1st shell	R (Ti-M)*	σ^2 2nd shell	R_{factor}
MP	0.95±0.13	2.75±0.01	1.98 ± 0.01	0.012 ± 0.003	3.61±0.06 3.82±0.06	0.016±0.013	0.01
MAl	0.98±0.12	0.5±1.0	1.98 ± 0.01	0.012 ± 0.003	3.72±0.06 3.95±0.06	0.016±0.011	0.01

*Two distinct Ti-M (M=Al,P) paths are necessary for the second shell fit.

From the first shell fit in Table 1 we have found that the average Ti-O bond distance is (1.98±0.01)Å. The average P/Al-O bond length reported by previous studies[21,49] on non substituted sieves is about 1.65Å confirming that the incorporation of Ti strongly deforms the

$AlPO_4$-5 framework. The fitted coordination number of Ti in TiALPO-5/act is 3.7±0.3 suggesting that we are in presence of a slightly defective material. Furthermore, it is worth noticing that the Ti-O bond distance in TiALPO-5/act is (0.19±0.02)Å longer than the one reported for an activated sample of TS-1.[50,51]

The study of the second shell using EXAFS cannot be conclusive because the best fit curves obtained do not allow distinguishing between the two models (see Figure 3c). On the contrary, vtc-XES can address this point.[36,52,53]

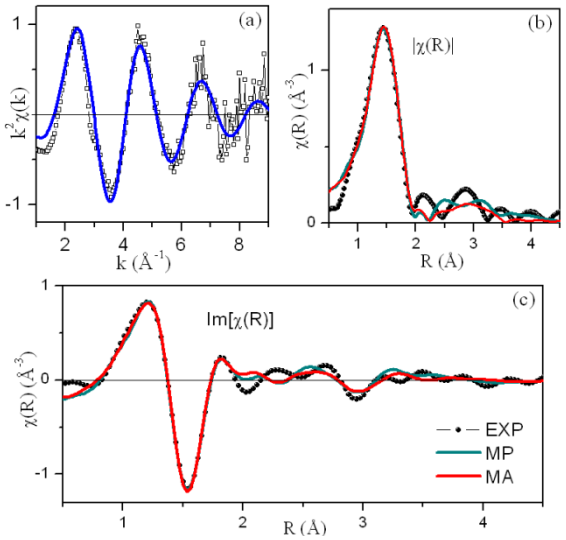

Figure 3. (a) Ti K-edge EXAFS of TiALPO-5/act with the calculated single shell Ti-O scattering path (1.98 Å). Module (b) and imaginary part (c) of the Fourier transformed best fit curves using ***MAl*** and ***MP*** clusters.

The comparison of the energy position of the Kβ" line (A) of the vtc-XES spectrum of TiAlPO-5/act and TS-1 presented in Figure 4a confirms the presence of O in the first shell of Ti. Furthermore the comparison of the Kβ" intensity in the two compounds suggests that the Ti-O bond length is longer for TiAlPO5 than for TS-1. Calculations on cluster modelling the Ti

environment in TS-1 as a function of the Ti-O (first shell) bond distance prove that spectral features decrease exponentially increasing the bond-length (see Figure 4b).

The $K\beta_{2,5}$ region of TS-1/act presents two main features B and C, arising from transitions involving σ and π molecular orbitals respectively, separated in energy according to the tetrahedral symmetry of the Ti sites.[37] As TS-1/act, also the $K\beta_{2,5}$ region of TiAlPO-5/act presents two main features. Their maximum is nearly at the same energy position observed for TS-1/act. It is worth noticing however that contrary to TS-1/act B is less intense than C (see Figure 4a). Furthermore we do think that the features of TiALPO-5 are less intense than in TS-1/act due to the increased Ti-O average bond distance. It is worth noticing that the comparison of the intensities of the vtc-XES spectra reported in Figure 5 can be done in a quantitative ground because of the normalization to the spectral area that includes the $K\beta$ main and the vtc lines, see Section 2.2.

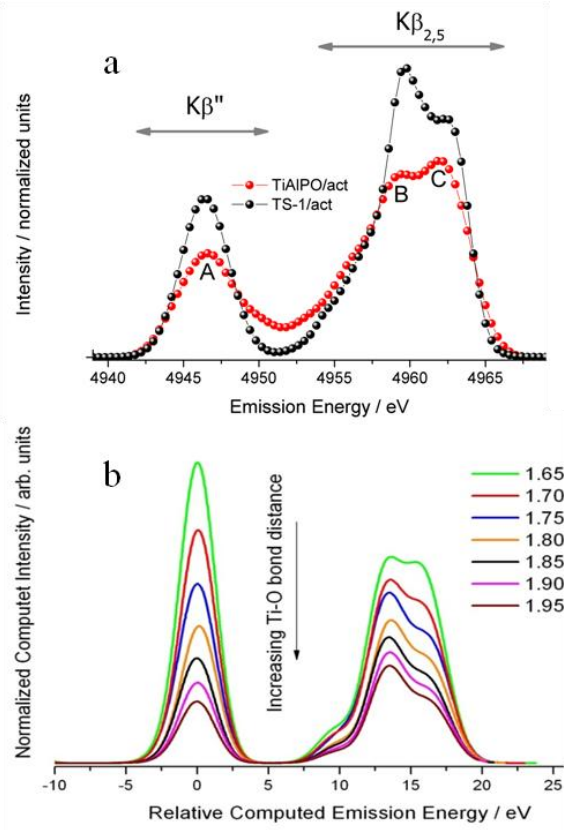

Figure 4. (a) Experimental vtc-XES spectra of TiALPO-5/act (red dots) and TS-1/act. (black dots). (b) Computed vtc-XES of a Ti centred cluster with Ti-O bond distance symmetrically increasing from 1.65Å to 1.95Å

To be more quantitative, we performed ground state DFT vtc-XES calculations shown in Figure 5 and based on ***MAl*** and **MP** models of Figure 1. We observe, for all functional, that the agreement of the calculations with the experimental spectrum is considerably better when Al in the second shell is considered (i.e. cluster ***MAl***). We conclude that in TiALPO-5/act a major fraction of Ti ions substitute the P sites.

Emission lines are connected to specific molecular orbitals (MO) present in the systems. As an example in Figure 5c the most relevant MO for the ***MAl*** model are reported. The A feature of

Kβ" is linked to a σ MO within the first neighbourhoods, while the B and C features of $K\beta_{2,5}$ are linked to σ and π orbitals involving second neighbourhoods, respectively.

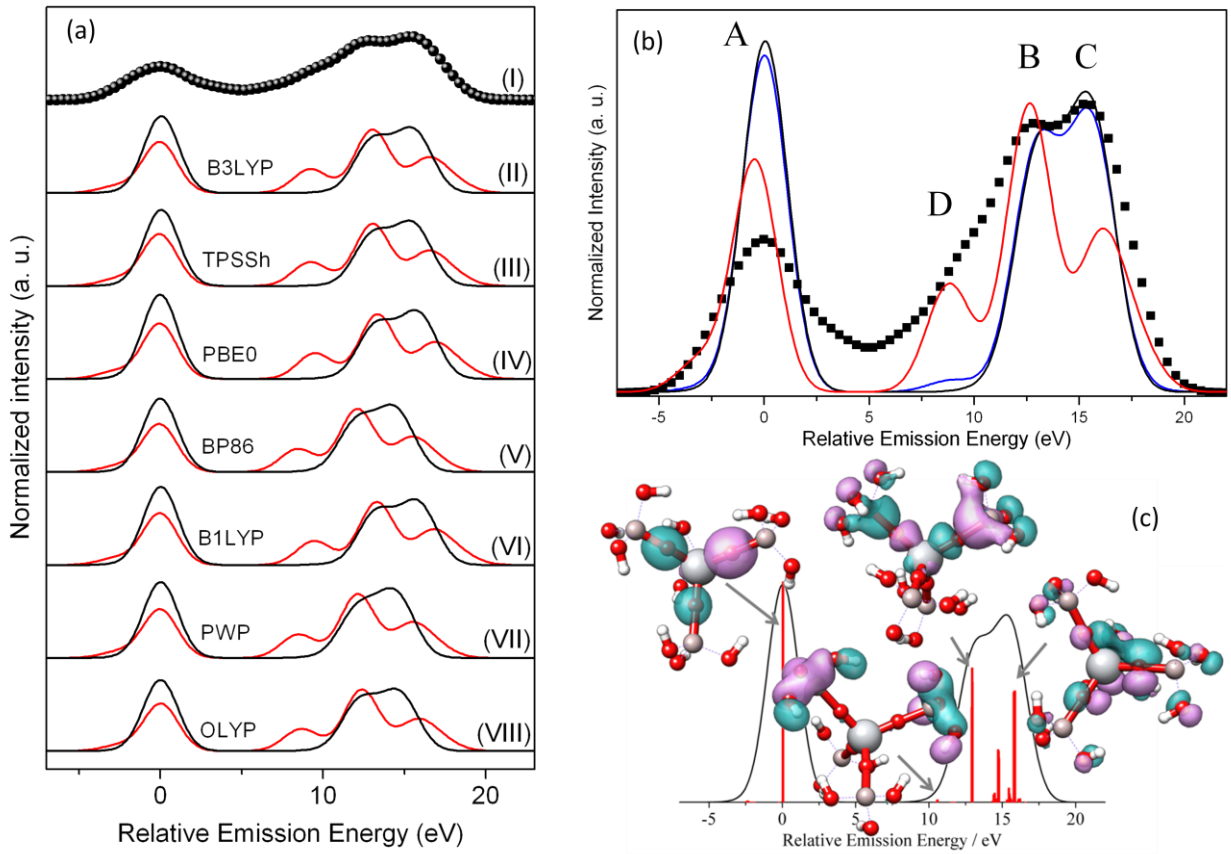

Figure 5. (a): vtc-XES spectra obtained from DFT calculations performed using clusters *MP* (red curve) and *MA* black curve) using various functional (II-VIII) compared with the experimental vtc-XES spectrum ofTiALPO-5/act (I). (b) Linear combination of calculated vtc-XES spectra with B3LYP functional (blue curve) from Mal (90%) and MP (10%) models of panel (a). (c): Representation of the calculated most important orbitals responsible for the vtc-XES signal using B3LYP functional with *MAl* cluster model.

It is well known that vtc-XES spectra can be used to identify the chemical nature of the first shell neighbours, also for elements lying in adjacent positions of the periodic table, because the

technique is sensible to the ligand 2s binding energy (rather than to the number of electrons Z as XAS is).[34,39] We remark that the B-C intensity ratio is affected by the charge lying on the second shell ligands as observed in the case of TS-1.[36,37] We then propose that vtc-XES can be also used to identify second shell ligands having similar atomic number values, *i.e.* in cases where EXAFS may fail because of the low Z contrast (13 and 15 for Al and P, respectively). Using linear combination of vtc-XES spectra, it is possible to more precisely quantify the amount of Ti which has replaced Al or P framework sites. The result of the best linear combination of spectra is shown in Figure 5b where a combination of (0.90±0.05)****MAl*** + (0.10±0.05)****MP*** has been used. Considering this linear combination we can also account for a part of the intensity of the shoulder at 7eV relative emission, which could not be explained with contribution only from more diffused MOs (see D feature in Figure 5c).[36] We conclude that with our approach sensitive to all Ti species present in the structure, the majority of Ti substitute P, but a not negligible amount, we estimated about 10±5%, substitutes Al. In the TiALPO-5/act formal Ti valence is (IV) for all species.

4 Conclusion

In our work we have outlined the architecture of the Ti(IV) sites within TiALPO-5/act combining X-ray absorption and X-ray emission spectroscopy with quantum mechanical calculations.

From EXAFS analysis we obtained a Ti-O average bond distance of (1.98±0.01)Å and an average Ti coordination number of (3.7±0.3), compatible with the expected 4-fold coordination resulting by an isomorphous substitution of Ti(IV) inside the ALPO-5 framework. As expected, the analysis of the second shell EXAFS signal did not allow distinguishing between Al or P occupancies. We then employed vtc-XES to address the problem. The finding is that the second

shell around Ti is for the majority composed of Al ligands, *i.e.* Ti substitute mainly P within TiALPO-5. From the linear combination method we more precisely assessed that 90±5% of Ti substitute P, but a not negligible amount, we estimated about 10±5%, substitutes Al. The bulk techniques employed, which is sensitive to all Ti in the framework, extends previous HYSCORE EPR evidences that were valid for the fraction of Ti ions reduced with H_2 which has been estimated, for their sample, to be 20±5%.[25] Note that in Ref. [26] a more severe reduction condition has been adopted (975 K) resulting in an higher fraction of reduced Ti species. Notwithstanding the slight discrepancy between the estimated percentages, both techniques point to a presence of (reducible) Ti ions at Al sites which should have an important role in the catalytic activity of the material, as they are the sites that clearly show modifications upon reduction.

Finally we notice that the increasing number of synchrotron light sources makes the approach here presented, *i.e.* combining EXAFS with vtc-XES, accessible for the large community of researchers interested in the characterization of materials.

Corresponding Authors

*erik.gallo@esrf.fr

*piovano@ill.fr

Acknowledgments

The European Synchrotron Radiation Facility (ESRF, Grenoble) is gratefully acknowledged for beamtime allocation.

Referencees

(1) Bellussi, G.; Pollesel, P. Industrial applications of zeolite catalysts: production and uses of light olefins. *Stud. Surf. Sci. Catal.* **2005**, *158*, 1201-1212.

(2) Danilczuk, M.; Dlugopolska, K.; Ruman, T.; Pogocki, D. Molecular Sieves in Medicine. *Mini Rev. Med. Chem.* **2008**, *8*, 1407-1417.

(3) Szostak, R. M., *Molecular Sieves*; Van Nostrand Reinhold: New York, **1989**.

(4) Vayssilov, G. N. Structural and physicochemical features of titanium silicalites. *Catal. Rev.-Sci. Eng.* **1997**, *39*, 209-251.

(5) Corma, A. State of the art and future challenges of zeolites as catalysts. *J. Catal.* **2003**, *216*, 298-312.

(6) Taramasso, M.; Perego, G.; Notari, B., **1983**, US Patent No. 4410501.

(7) Notari, B. Microporous crystalline titanium silicates. *Adv. Catal.* **1996**, *41*, 253.

(8) Bordiga, S.; Bonino, F.; Damin, A.; Lamberti, C. Reactivity of Ti(IV) species hosted in TS-1 towards H_2O_2-H_2O Solutions investigated by ab initio cluster and periodic approaches combined with experimental XANES and EXAFS data: a review and new highlights. *Phys. Chem. Chem. Phys.* **2007**, *9*, 4854-4878.

(9) Perego, C.; Carati, A.; Ingallina, P.; Mantegazza, M. A.; Bellussi, G. Production of titanium containing molecular sieves, and their application in catalysis. *Appl. Catal. A-Gen.* **2001**, *221*, 63-72.

(10) Blasco, T.; Camblor, M. A.; Corma, A.; Esteve, P.; Guil, J. M.; Martinez, A.; Perdigon-Melon, J. A.; Valencia, S. Direct synthesis and characterization of hydrophobic aluminum-free Ti-beta zeolite. *J. Phys. Chem. B* **1998**, *102*, 75-88.

(11) Eilertsen, E. A.; Bordiga, S.; Lamberti, C.; Damin, A.; Bonino, F.; Arstad, B.; Svelle, S.; Olsbye, U.; Lillerud, K. P. Synthesis of Titanium Chabazite: A New Shape Selective Oxidation Catalyst with Small Pore Openings and Application in the Production of Methyl Formate from Methanol. *Chemcatchem* **2011**, *3*, 1869-1871.

(12) Eilertsen, E. A.; Giordanino, F.; Lamberti, C.; Bordiga, S.; Damin, A.; Bonino, F.; Olsbye, U.; Lillerud, K. P. Ti-STT: a new zeotype shape selective oxidation catalyst. *Chem. Commun.* **2011**, *47*, 11867-11869.

(13) Wu, P.; Kubota, Y.; Yokoi, T. A Career in Catalysis: Takashi Tatsumi. *ACS Catal.* **2014**, *4*, 23-30.

(14) Wilson, S. T.; Lok, B. M.; Messina, C. A.; Cannan, T. R.; Flanigen, E. M., *Aluminophosphate Molecular Sieves: A New Class of Microporous Crystalline Inorganic Solids*, in: Intrazeolite Chemistry, **1983**.

(15) Akolekar, D. B. Acidity and Catalytic Properties of AlPO4-11, SAPO-11, MAPO-11, NiAPO-11, MnAPO-11 and MnAPSO-11 Molecular-Sieves. *J. Mol. Catal. A* **1995**, *104*, 95-102.

(16) Bhat, S. D.; Mallikarjuna, N. N.; Aminabhavi, T. M. Microporous alumino-phosphate (AlPO4-5) molecular sieve-loaded novel sodium alginate composite membranes for pervaporation dehydration of aqueous-organic mixtures near their azeotropic compositions. *J. Membrane Sci.* **2006**, *282*, 473-483.

(17) Chen, Y. Y.; Huang, Y. L.; Xiu, J. H.; Han, X. W.; Bao, X. H. Direct synthesis, characterization and catalytic activity of titanium-substituted SBA-15 mesoporous molecular sieves. *Appl. Catal. A-Gen.* **2004**, *273*, 185-191.

(18) Gao, Q. M.; Weckhuysen, B. M.; Schoonheydt, R. A. On the synthesis of CoAPO-46, -11 and -44 molecular sieves from a Co(Ac)(2) 4H(2)O Al(iPrO)(3) Pr2NH H2O gel via experimental design. *Micropor. Mesopor. Mat.* **1999**, *27*, 75-86.

(19) Haanepen, M. J.; vanHooff, J. H. C. VAPO as catalyst for liquid phase oxidation reactions .1. Preparation, characterisation and catalytic performance. *Appl. Catal. A-Gen.* **1997**, *152*, 183-201.

(20) Holland, B. T.; Isbester, P. K.; Blanford, C. F.; Munson, E. J.; Stein, A. Synthesis of ordered aluminophosphate and galloaluminophosphate mesoporous materials with anion-exchange properties utilizing polyoxometalate cluster/surfactant salts as precursors. *J. Am. Chem. Soc.* **1997**, *119*, 6796-6803.

(21) Hsu, B. Y.; Cheng, S.; Chen, J. M. Synthesis and catalytic properties of Ti-substituted SAPO molecular sieves. *J. Mol. Catal. A-Chem.* **1999**, *149*, 7-23.

(22) Chen, L.-H.; Li, X.-Y.; Tian, G.; Li, Y.; Rooke, J. C.; Zhu, G.-S.; Qiu, S.-L.; Yang, X.-Y.; Su, B.-L. Highly Stable and Reusable Multimodal Zeolite TS-1 Based Catalysts with Hierarchically Interconnected Three-Level Micro–Meso–Macroporous Structure. *Angew. Chem. Int. Ed.* **2011**, *50*, 11156-11161.

(23) Sheldon, R. A. Redox molecular sieves as heterogeneous catalysts for liquid phase oxidations. *Stud. Surf. Sci. Catal.* **1997**, *110*, 151-175.

(24) Akolekar, D. B.; Ryoo, R. Titanium incorporated ATS and AFI type aluminophosphate molecular sieves. *J. Chem. Soc., Faraday Trans.* **1996**, *92*, 4617-4621.

(25) Maurelli, S.; Vishnuvarthan, M.; Chiesa, M.; Berlier, G.; Van Doorslaer, S. Elucidating the Nature and Reactivity of Ti Ions Incorporated in the Framework of AlPO-5 Molecular Sieves. New Evidence from 31P HYSCORE Spectroscopy. *J. Am. Chem, Soc.* **2011**, *133*, 7340-7343.

(26) Maurelli, S.; Vishnuvarthan, M.; Berlier, G.; Chiesa, M. NH3 and O2 interaction with tetrahedral Ti3+ ions isomorphously substituted in the framework of TiAlPO-5. A combined pulse EPR, pulse ENDOR, UV-Vis and FT-IR study. *Phys. Chem. Chem. Phys.* **2012**, *14*, 987-995.

(27) Prakash, A. M.; Kevan, L.; Zahedi-Niaki, M. H.; Kaliaguine, S. Electron spin resonance and electron spin-echo modulation evidence for the isomorphous substitution of titanium in titanium aluminophosphate molecular sieves. *J. Phys. Chem. B* **1999**, *103*, 831-837.

(28) Prakash, A. M.; Kurshev, V.; Kevan, L. Electron spin resonance and electron spin echo modulation evidence for the isomorphous substitution of Ti in TAPO-5 molecular sieve. *J. Phys. Chem. B* **1997**, *101*, 9794-9799.

(29) Elanany, M.; Vercauteren, D. P.; Kubo, M.; Miyamoto, A. The acidic properties of H-MeAlPO-5 (Me = Si, Ti, or Zr): A periodic density functional study. *J. Mol. Catal. A-Chem.* **2006**, *248*, 181-184.

(30) Cora, F.; Catlow, C. R. A. Ionicity and framework stability of crystalline aluminophosphates. *J. Phys. Chem. B* **2001**, *105*, 10278-10281.

(31) Rehr, J. J.; Albers, R. C. Theoretical approaches to x-ray absorption fine structure. *Rev. Mod. Phys.* **2000**, *72*, 621-654.

(32) Mino, L.; Agostini, G.; Borfecchia, E.; Gianolio, D.; Piovano, A.; Gallo, E.; Lamberti, C. Low-dimensional systems investigated by x-ray absorption spectroscopy: a selection of 2D, 1D and 0D cases. *J. Phys. D-Appl. Phys.* **2013**, *46*.

(33) Bordiga, S.; Groppo, E.; Agostini, G.; van Bokhoven, J. A.; Lamberti, C. Reactivity of Surface Species in Heterogeneous Catalysts Probed by In Situ X-ray Absorption Techniques. *Chem. Rev.* **2013**, *113*, 1736-1850.

(34) Bergmann, U.; Horne, C. R.; Collins, T. J.; Workman, J. M.; Cramer, S. P. Chemical dependence of interatomic X-ray transition energies and intensities - a study of Mn K beta " and K beta(2,5) spectra. *Chem. Phys. Lett.* **1999**, *302*, 119-124.

(35) Smolentsev, G.; Soldatov, A. V.; Messinger, J.; Merz, K.; Weyhermuller, T.; Bergmann, U.; Pushkar, Y.; Yano, J.; Yachandra, V. K.; Glatzel, P. X-ray Emission Spectroscopy To Study Ligand Valence Orbitals in Mn Coordination Complexes. *J. Am. Chem. Soc.* **2009**, *131*, 13161-13167.

(36) Gallo, E.; Lamberti, C.; Glatzel, P. Investigation of the valence electronic states of Ti(iv) in Ti silicalite-1 coupling X-ray emission spectroscopy and density functional calculations. *Phys. Chem. Chem. Phys.* **2011**, *13*, 19409-19419.

(37) Gallo, E.; Bonino, F.; Swarbrick, J. C.; Petrenko, T.; Piovano, A.; Bordiga, S.; Gianolio, D.; Groppo, E.; Neese, F.; Lamberti, C.; Glatzel, P. Preference towards Five-Coordination in Ti Silicalite-1 upon Molecular Adsorption. *ChemPhysChem* **2012**, *14*, 79-83.

(38) Hamalainen, K.; Siddons, D. P.; Hastings, J. B.; Berman, L. E. Elimination of the Inner-Shell Lifetime Broadening in X-Ray-Absorption Spectroscopy. *Phys. Rev. Lett.* **1991**, *67*, 2850-2853.

(39) Glatzel, P.; Bergmann, U. High resolution 1s core hole X-ray spectroscopy in 3d transition metal complexes - electronic and structural information. *Coord. Chem. Rev.* **2005**, *249*, 65-95.

(40) Ravel, B.; Newville, M. ATHENA, ARTEMIS, HEPHAESTUS: data analysis for X-ray absorption spectroscopy using IFEFFIT. *J. Synchrot. Radiat.* **2005**, *12*, 537-541.

(41) Lamberti, C.; Bordiga, S.; Arduino, D.; Zecchina, A.; Geobaldo, F.; Spano, G.; Genoni, F.; Petrini, G.; Carati, A.; Villain, F.; Vlaic, G. Evidence of the presence of two different framework Ti(IV) species in Ti-silicalite-1 in vacuo conditions: an EXAFS and a photoluminescence study. *J. Phys. Chem. B* **1998**, *102*, 6382-6390.

(42) Ankudinov, A. L.; Ravel, B.; Rehr, J. J.; Conradson, S. D. Real-space multiple-scattering calculation and interpretation of x-ray-absorption near-edge structure. *Phys. Rev. B* **1998**, *58*, 7565-7576.

(43) Ricchiardi, G.; Damin, A.; Bordiga, S.; Lamberti, C.; Spano, G.; Rivetti, F.; Zecchina, A. Vibrational structure of titanium silicate catalysts. A spectroscopic and theoretical study. *J. Am. Chem. Soc.* **2001**, *123*, 11409-11419.

(44) Damin, A.; Bordiga, S.; Zecchina, A.; Lamberti, C. Reactivity of Ti(IV) sites in Ti-zeolites: An embedded cluster approach. *J. Chem. Phys.* **2002**, *117*, 226-237.

(45) Neese, F. The ORCA program system. *WIREs* **2012**, *2*, 73-78.

(46) Jensen, K. P. Bioinorganic Chemistry Modeled with the TPSSh Density Functional. *Inorg. Chem.* **2008**, *47*, 10357-10365.

(47) Pettersen, E. F.; Goddard, T. D.; Huang, C. C.; Couch, G. S.; Greenblatt, D. M.; Meng, E. C.; Ferrin, T. E. UCSF Chimera—A visualization system for exploratory research and analysis. *J. Comput. Chem.* **2004**, *25*, 1605-1612.

(48) Glatzel, P.; Weng, T.-C.; Kvashnina, K.; Swarbrick, J.; Sikora, M.; Gallo, E.; Smolentsev, N.; Mori, R. A. Reflections on hard X-ray photon-in/photon-out spectroscopy for electronic structure studies. *J. Electron Spectrosc.* **2013**, *188*, 17-25.

(49) Meier, W. M.; Olson, D. H.; Baerlocher, C., *Atlas of Zeolite Structure Types*; Elsevier: London, **1996**.

(50) Bordiga, S.; Boscherini, F.; Coluccia, S.; Genoni, F.; Lamberti, C.; Leofanti, G.; Marchese, L.; Petrini, G.; Vlaic, G.; Zecchina, A. XAFS study of Ti-silicalite: structure of framework Ti(IV) in presence and in absence of reactive molecules (H_2O, NH_3). *Catal. Lett.* **1994**, *26*, 195-208.

(51) Bordiga, S.; Coluccia, S.; Lamberti, C.; Marchese, L.; Zecchina, A.; Boscherini, F.; Buffa, F.; Genoni, F.; Leofanti, G.; Petrini, G.; Vlaic, G. XAFS study of Ti-silicalite: structure of framework Ti(IV) in presence and absence of reactive molecules (H_2O, NH_3) and comparison with Ultraviolet-Visible and IR results. *J. Phys. Chem.* **1994**, *98*, 4125-4132.

(52) Lancaster, K. M.; Roemelt, M.; Ettenhuber, P.; Hu, Y.; Ribbe, M. W.; Neese, F.; Bergmann, U.; DeBeer, S. X-ray Emission Spectroscopy Evidences a Central Carbon in the Nitrogenase Iron-Molybdenum Cofactor. *Science* **2011**, *334*, 974-977.

(53) Safonov, V. A.; Vykhodtseva, L. N.; Polukarov, Y. M.; Safonova, O. V.; Smolentsev, G.; Sikora, M.; Eeckhout, S. G.; Glatzel, P. Valence-to-core X-ray emission spectroscopy identification of carbide compounds in nanocrystalline Cr coatings deposited from Cr(III) electrolytes containing organic substances. *J. Phys. Chem. B* **2006**, *110*, 23192-23196.